STM JOURNALS

Journal of
Polymer & Composites

ISSN: 2321-2810 (Online)
ISSN: 2321-8525 (Print)
Volume 13, Issue 2, 2025
DOI (Journal): 10.37591/JoPC

https://journals.stmjournals.com/JOPC/

Research JoPC

Current-Voltage Characteristics of 15-Atom Agnrs and Zcnts at Various Bias Voltages: Insights for Polymer Nanocomposite Applications

Anabathula Udaya Sri[1,*], D. Vinay Kumar[2]

Abstract

The present research investigates the electronic properties of 15-atom Armchair Graphene Nanoribbons (AGNRs) and 15-atom Zig-Zag Carbon Nanotubes (ZCNTs) under applied bias voltages of 100, 200, 300, 400, 500, and 600 millivolts. Using the Non-Equilibrium Green's Function (NEGF) technique, the study analyzes various electrical features, including current-voltage (I-V) characteristics, to understand the behavior of these nanostructures. The findings reveal that AGNRs exhibit a larger bandgap than ZCNTs, which have a zero-bandgap configuration, enabling improved control over electrical current flow. AGNRs demonstrate linear I-V behavior at 100 mV and 200 mV, while higher bias voltages (300 mV–600 mV) result in constant current flow. Conversely, ZCNTs display linear I-V behavior at lower voltages (100 mV–200 mV), with peak current flow observed around 300 mV. Beyond this, ZCNTs show decreasing current flow at higher voltages due to strong electron-electron interactions and quantum confinement effects Furthermore, embedding these nanostructures into polymer composites provides opportunities to harness their unique electronic properties for applications in flexible electronics, electromagnetic shielding, and energy storage. The study enhances our understanding of AGNRs and ZCNTs, offering promising insights for their integration into nanoelectronics devices.

Keywords: Nanostructures, NEGF, ZCNT, AGNR, I-V characteristics, polymer nanocomposites, flexible electronics, quantum confinement

INTRODUCTION

The remarkable advancements in nanotechnology have brought carbon-based nanostructures, such as Graphene Nanoribbons (GNRs) and Carbon Nanotubes (CNTs), into the spotlight as essential building blocks for next-generation nanoelectronic devices [1]. Their unique mechanical, electrical, and thermal properties, combined with their nanoscale dimensions, enable the development of highly efficient, compact systems suitable for diverse applications.

***Author for Correspondence**
Anabathula Udaya Sri
E-mail: udayasrivfstr@gmail.com

[1] Research Scholar, Department of Mechanical Engineering, Vignan's Foundation for Science, Technology and Research, Vadlamudi, Andhra Pradesh, India
[2] Associate professor, Department of Mechanical Engineering, Vignan's Foundation for Science, Technology and Research, Vadlamudi, Andhra Pradesh, India

Received Date: December 10, 2024
Accepted Date: January 13, 2025
Published Date: January 22, 2025

Citation: Anabathula Udaya Sri, D. Vinay Kumar. Current-Voltage Characteristics of 15-Atom AGNRs and ZCNTs at Various Bias Voltages: Insights for Polymer Nanocomposite Applications. Journal of Polymer & Composites. 2025; 13 (2): 135–144p.

Armchair Graphene Nanoribbons (AGNRs)

Among the various forms of GNRs, Armchair Graphene Nanoribbons (AGNRs) are particularly notable for their tunable electronic properties, driven by edge states and a distinct bandgap. These characteristics make AGNRs a preferred choice for applications in transistors, sensors, and other nanoelectronic components. Previous studies have demonstrated that AGNRs' bandgap can be engineered by modifying their width and edge structures, offering control over their electronic

behavior. However, the behavior of AGNRs under non-equilibrium conditions, such as bias voltage, is still inadequately understood, especially in the presence of defects. Addressing these gaps is crucial for optimizing AGNR performance in practical applications [2].

Zig-Zag Carbon Nanotubes (ZCNTs)

Carbon Nanotubes (CNTs), particularly Zig-Zag Carbon Nanotubes (ZCNTs), represent another promising class of nanostructures with unique edge-localized states [3]. These states, characterized by non-bonding orbitals near the Fermi energy level, impart ZCNTs with distinct electronic and mechanical properties. ZCNTs exhibit a variety of behaviors depending on their curvature and chirality, making them versatile candidates for applications in nanocircuits, mechanical nanosprings, and energy devices. However, their response to higher bias voltages, especially in comparison to AGNRs, requires further investigation to fully harness their potential in nanoelectronics.

Polymer Nanocomposites: A Synergistic Approach

To unlock their full potential, AGNRs and ZCNTs are often embedded into polymer matrices, forming nanocomposites that synergize the exceptional properties of nanostructures with the processability, flexibility, and durability of polymers [4]. These composites open new avenues for flexible electronics, energy storage, and electromagnetic interference (EMI) shielding applications.

Role of Nanostructures in Polymer Matrices

Incorporating AGNRs and ZCNTs into polymers enhances the electrical conductivity, mechanical strength, and thermal stability of the resulting composite material. The tunable bandgap of AGNRs allows precise control over charge transport within the polymer matrix, making the composites ideal for high-performance electronic applications. Similarly, ZCNTs provide robust mechanical reinforcement and exceptional conductivity, further elevating the performance of polymer nanocomposites [5].

Processing and Fabrication Techniques

Fabrication methods for AGNR- and ZCNT-based polymer composites include:

- *Solution blending*: Ensures uniform dispersion of nanostructures within the polymer.
- *Melt compounding:* Combines nanostructures with thermoplastics for scalable production.
- In-*situ polymerization*: Integrates nanostructures during polymer formation, enabling strong interfacial bonding.

These techniques ensure optimized interactions between the nanostructures and the polymer matrix, enhancing the composite's overall mechanical and electrical properties [6].

Applications in Flexible Electronics and Energy Storage

- *Flexible electronics:* The high flexibility and conductivity of AGNR and ZCNT composites make them suitable for wearable devices and other portable electronics.
- *Energy storage*: Enhanced electron transport in these composites enables their use in high-performance supercapacitors and batteries.
- *EMI shielding:* These materials' high conductivity and mechanical robustness provide effective shielding against electromagnetic interference, a critical requirement for modern electronic systems.

Non-Equilibrium Green's Function (NEGF) Method

This research employs the non-equilibrium Green's function (NEGF) method to explore the electronic transport properties of AGNRs and ZCNTs. NEGF provides a theoretical framework to analyze nanoscale systems' response to external perturbations, such as bias voltages. The approach is instrumental in studying key electronic characteristics, including transmission, energy-momentum relationships, and current-voltage (I-V) behaviour [7].

Research Objective

This study focuses on understanding the behavior of 15-atom Armchair Graphene Nanoribbons (AGNRs) and 15-atom Zig-Zag Carbon Nanotubes (ZCNTs) under bias voltages of 100 mV to 600 mV. By employing the NEGF method, the research examines their current-voltage (I-V) characteristics and compares their electronic properties. Furthermore, integrating these nanostructures into polymer composites is discussed to highlight their potential in flexible electronics, energy storage, and other advanced applications.

This comprehensive analysis bridges the knowledge gap related to the non-equilibrium behavior of AGNRs and ZCNTs, paving the way for their efficient use in future nanoelectronic and composite-based technologies.

METHODOLOGY

The I-V properties of Armchair Graphene Nano Ribbons (AGNRs) and Zig-zag Carbon Nano Tubes (ZCNTs) are studied through a series of processes using Non-Equilibrium Green, which are explained here The Armchair Graphene Nano Ribbon (AGNR) and Zig-zag Carbon Nano Tubes (ZCNTs) are first modeled employing a strict binding Hamiltonian in this methodology. This Hamiltonian considers the nearest-neighbor relationships between carbon atoms inside the honeycomb structure to analyze the interactions between them in the graphene lattice. This Hamiltonian scattering area, which is made up of ZCNTs and AGNRs connected for semi-infinite leads, has been formed [8-10].

These leads stand in for the source and drain electrodes. It is significant to note that this study has assumed that the channel's material and the source and drain leads are the same, Creating Non-Equilibrium Green's Function equations is the next stage [11]. The equations describing the relationship between the scattering zone and the leads (the source and drain electrodes) can be found by integrating the Hamiltonian with self-energy functions. Understanding the relationship between the AGNR and ZCNTs and the electrodes requires an understanding of their self-energy functions. Subsequently, numerical techniques are utilized to solve NEGF problems, especially the iterative Green's function method. We can determine the current-voltage characteristics of Zig-zag Carbon Nano Tubes (ZCNTs) and Armchair Graphene Nano Ribbon (AGNR) tubes to this numerical solution.

Proceeding to the third stage, we compare the accuracy and reliability of the NEGF method with data obtained from other theoretical approaches. Specifically, we examine at how our results match those obtained from other ways.

The final step investigates how different factors impact the electronic properties of Armchair Graphene Nano Ribbons (AGNRs) and Zig-zag Carbon Nanotubes (ZCNTs) when subjected to bias voltages of 50 millivolts, 150 millivolts, and 300 millivolts. These factors include the width, length, bias voltage, temperature, and doping level of AGNRs and ZCNTs [12]. However, it's essential to emphasize that the primary focus of this paper remains on their behavior regarding current-voltage (I-V) characteristics. Thoroughly analyzing various electronic attributes of both AGNRs and ZCNTs, we utilize the Non-Equilibrium Green's Function method, to explore current-voltage characteristics.

Expression for the calculation of quantum wave (Ψ) for any type of particle such as an electron (Schrodinger equation)

$$i\hbar \frac{\partial}{\partial t}\Psi(r,t) = \left[\frac{-\hbar^2}{2m}\nabla^2 + V(r,t)\right]\Psi(r,t) \quad (1)$$

Expression for the calculation of quantum wave (Ψ) for Time Independent particle (Time Independent Schrodinger Equation)

$$\left[\frac{-\hbar^2}{2m}\nabla^2 + V(r)\right]\Psi(r) = E\Psi(r) \quad (2)$$

Expression for the calculation of quantum wave (Ψ) for free electrons

$$\frac{-\hbar^2}{2m}\nabla^2\Psi(r) = E\Psi(r) \quad (3)$$

By solving he above obtained equation here gets the function

$$\Psi = A\cos\left(\frac{2\pi}{\lambda}x\right) \quad (4)$$

Expression for Green's Function

$$G(E) = (EI - H - \Sigma_L - \Sigma_R)^{-1} \quad (5)$$

Channel current-calculation Expression

$$I_{LR} = \int_{-\infty}^{\infty}\frac{e}{h}T(E)(f_L - f\ )dE \quad (6)$$

Fermi level energy Expression

$$f = \frac{1}{1+e^{\frac{E-E_F}{kT}}} \quad (7)$$

Expression for property of transmission

$$T(E) = \text{tran}(\Gamma_L G(E)\Gamma_R G^*(E)) \quad (8)$$

Expression of Green's Function

$$G(E) = (EI - H - \Sigma_L - \Sigma_R)^{-1} \quad (9)$$

Self-energy Expression

$$\Sigma = \tau g \tau^+ \quad (10)$$

E-K Diagram for Free Electron

E = energy of an electron, K = wave vector, for free electron the Potential Energy is zero K.E + P.E = T.E, Hence K.E = T.E

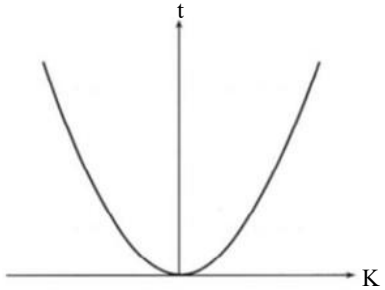

Figure 1. E-K diagram for free electron [13].

$$E = \frac{h^2 k^2}{2m} \tag{11}$$

$$H\Psi = E\Psi \tag{12}$$

Figure 1 represents the relationship between electron energy and velocity as the wave vector (K) of free electrons ranges from "0" to "∞." Consequently, this transition in wave vector leads to a corresponding shift in energy (E) from "0" to "∞." This graphical representation is commonly referred as the Energy-Momentum (E-K) diagram, E-K diagram is a valuable tool that offers an understanding of the permissible energy levels and the associated momentum of electrons at specific energy states E-K diagram also provides information about a material's structural characteristics indicating whether a material behaves like a semiconductor or a metal [14]. It provides information on whether the material's band gap is direct or indirect. While one approach to determining the band gap involves extracting it directly from the E-K diagram, it can also be determined by analyzing the material's electronic characteristics. The simplification of the time-independent equation is a helpful step in gaining these valuable insights [15].

RESULTS AND DISCUSSION

Figure 2 provides a representation of the atomic arrangement of both 15-atom AGNR and ZCNT under a honeycomb configuration. Here, AGNR exhibits a width of 1.72nm, whereas ZCNT has a width of 0.48 nm. Comparing both materials with the same number of atoms shows an interesting fact that the ribbon width of armchair graphene nanoribbons (AGNRs) is significantly bigger than that of zig-zag carbon nanotubes (ZCNTs) [16].

Figure 3 represents the band structure for 15-atom Armchair Graphene Nanoribbons (AGNRs) and Zig-zag Carbon Nanotubes (ZCNTs) having armchair edges, displayed in the Energy-Momentum (E-K) diagram, simply and attractively. Two different bands are shown in the diagram, separated apart by a band gap. The upper set is composed of conduction bands, which aren't fully occupied by electrons, and the lower set is composed of valence bands, which are completely occupied by electrons. The obtained band gap values are 0.37 eV for 15-atom AGNRs and 0.00 eV for ZCNTs. This band gap measures the energy necessary to transmit electrons from the valence band to the conduction band and has a significant impact on the electrical characteristics of ZCNTs and AGNRs.

The band structure of 15-atom AGNRs and ZCNTs with armchair edges shows a significant band gap. This band gap arises because of quantum confinement effects. This study reveals that when comparing materials with the same number of atoms, the bandgap in zig-zag Carbon Nanotubes (ZCNTs) is significantly narrower than that of armchair graphene nanoribbons (AGNRs). It means that the energy required for the transmission of electrons from the valence band to the conduction band is lesser in ZCNTs than in AGNRs [17].

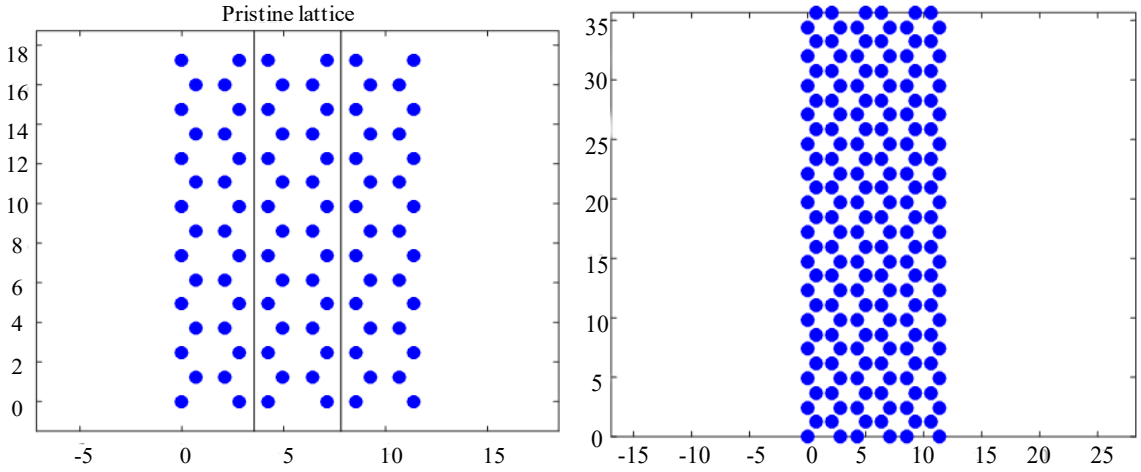

Figure 2. Pristine lattice of 15-AGNR and ZCNT honeycomb structure.

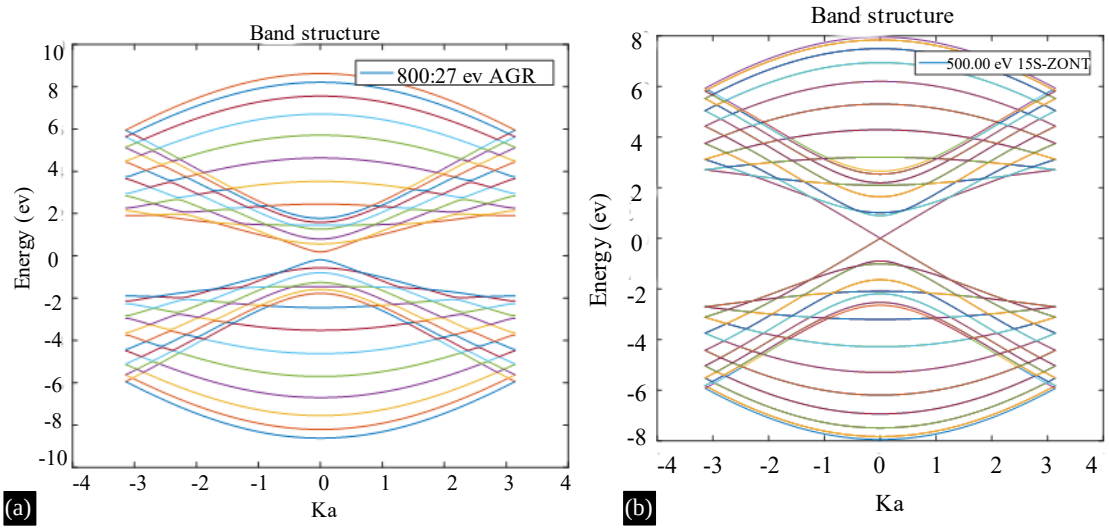

Figure 3. Energy-momentum (E-K) diagrams of 15-atom AGNR&ZCNT (a)15 AGNR, (b) 15-ZCNT

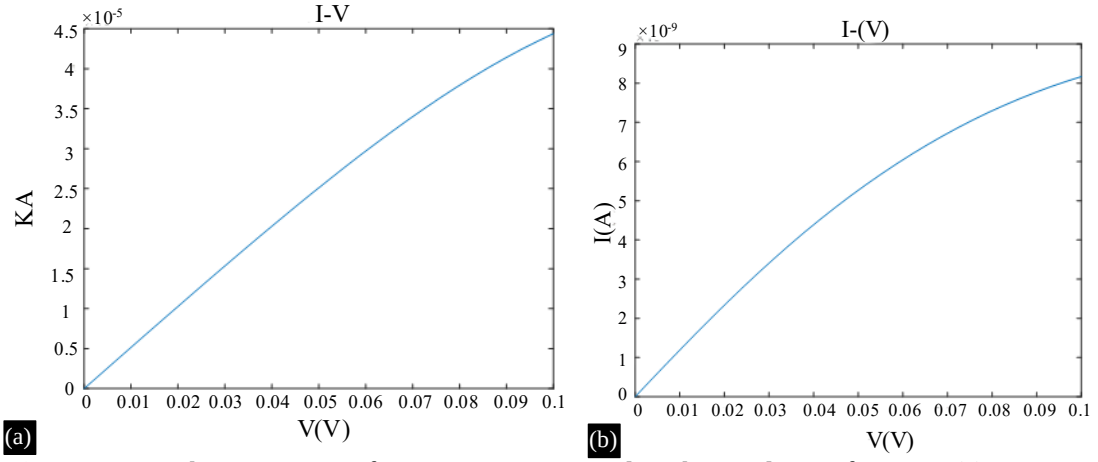

Figure 4. I-V Characteristics of 15-atom AGNRs under a bias voltage of 100Mv (a) 15-AGNR, (b) 15-ZCNT

Figure 4 represents under a bias voltage of 100mV, a current passing through both AGNRs and ZCNTs increases from zero as a voltage is applied. Current-voltage characteristics of AGNRs and ZCNTs exhibit linear behavior when subjected to a 100-millivolt, reaching a point of saturation where the current levels off. Saturation current is constrained by an available reachable number of conducting states in AGNRs and ZCNTs. ZCNTs show a larger current for 100mV voltage than that of AGNRs. A larger carrier concentration is shown by the I-V trends in Figure 4, which show a steeper I-V curve and a higher saturation current [18].

Figure 5 illustrates the current-voltage behavior in 15-atom Armchair Graphene Nanoribbons (AGNRs) and 15-atom Zig-zag Carbon Nanotubes (ZCNTs) under 200mV bias voltage. As the voltage is applied, both the 15-atom AGNR and ZCNT exhibit rapid increase in current from zero. These specific AGNRs and ZCNTs exhibit linear current-voltage (I-V) characteristics initially when subjected to a 200-millivolt bias, finally reaches a saturation point where the current stabilizes. Saturation current is primarily determined by available conducting states within AGNRs and ZCNTs. However, beyond this saturation point, AGNRs and ZCNTs maintain a constant current. We can observe an increase in currents in both AGNRs and ZCNTs as voltages increased from 100mV TO 200Mv.This pattern can be attributed to a greater carrier concentration and the possibility of a band gap in the structures of AGNRs and ZCNTs. It also relates with the steeper I-V curve and higher saturation current noted in both sets of I-V plots [19].

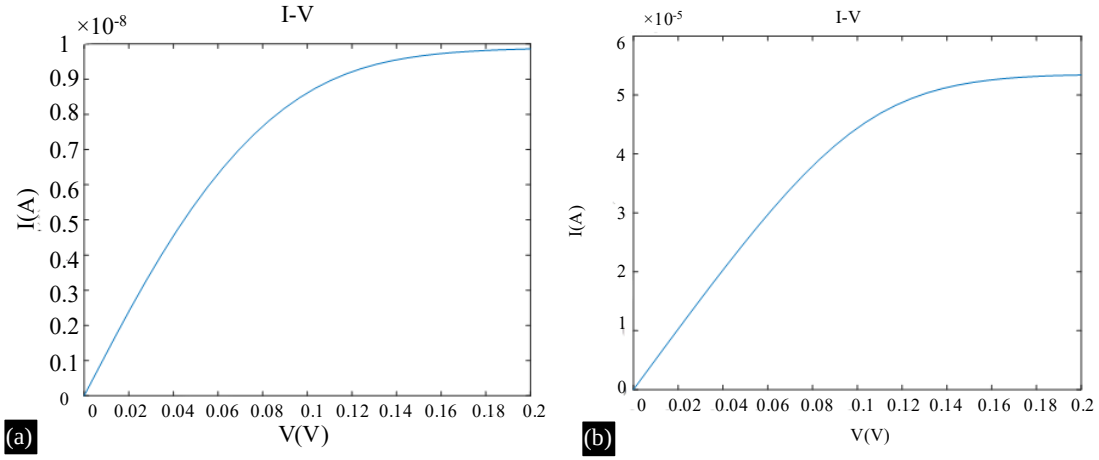

Figure 5. I-V Characteristics of 15-atom AGNR's and ZCNT's under a bias voltage of 200mV (a) 15-AGNR, (b) 15-ZCNT

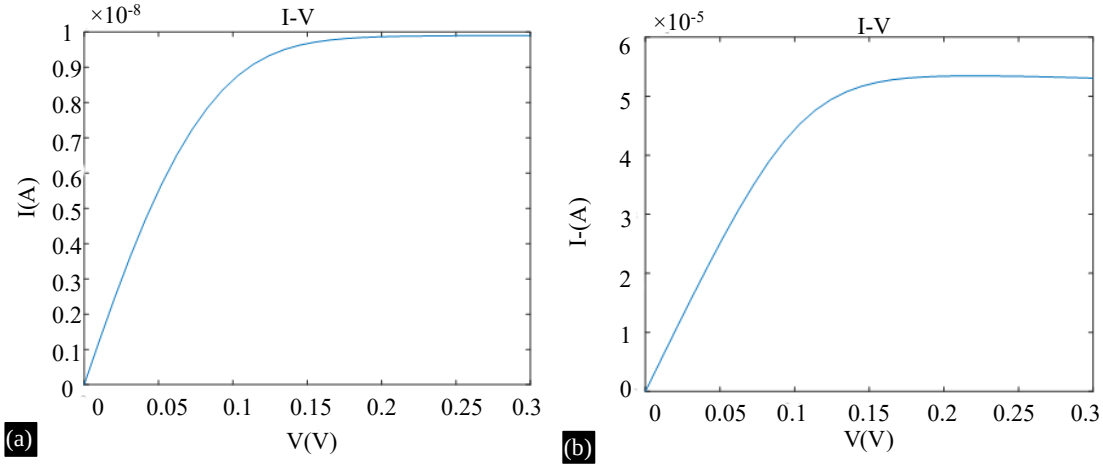

Figure 6. I-V Characteristics of 15-atom AGNRs and ZCNTs under a bias voltage of 300mV (a) 15-AGNR, (b) 15-ZCNT.

Figure 6 represents how the current behaves in 15-atom Armchair Graphene Nanoribbons (AGNRs) and 15-atom Zig-zag Carbon Nanotubes (ZCNTs) under a bias voltage of 300mV. As the voltage is applied, the current initially increases from zero for both the 15-atom AGNR and ZCNT. For these both sets of I-V graphs are shown in Fig. 6 and is explained by the presence of a band gap and higher carrier concentration in the structures of ZCNTs and AGNRs. Here we can observe no change in current with increase of voltage from 200mV TO 300 mV in both AGNRs and ZCNTs [20].

Figure 7 represents how the current behaves in 15-atom Armchair Graphene Nanoribbons (AGNRs) and 15-atom Zig-zag Carbon Nanotubes (ZCNTs) under a bias voltage of 400mV. As the voltage is applied, the current initially increases from zero for both the 15-atom AGNR and ZCNT. For these specific 15-atom AGNRs and ZCNTs, the current-voltage (I-V) characteristics display a linear behavior when subjected to a 400-millivolt bias, after reaching saturation point, the current stabilizes. This saturation current is primarily determined by available conducting states within the AGNRs and ZCNTs. However, after reaching this saturation point, AGNRs maintain a constant current, while ZCNTs exhibit a decrease in current or a reduction in the I-V curve as the voltage increases from 300mV to 400mV [21]. This result corresponds with the steeper I-V curve and greater saturation current observed in both sets of I-V graphs shown in Figure 7 and is explained by the presence of a band gap and higher carrier concentration in the structures of ZCNTs and AGNRs.

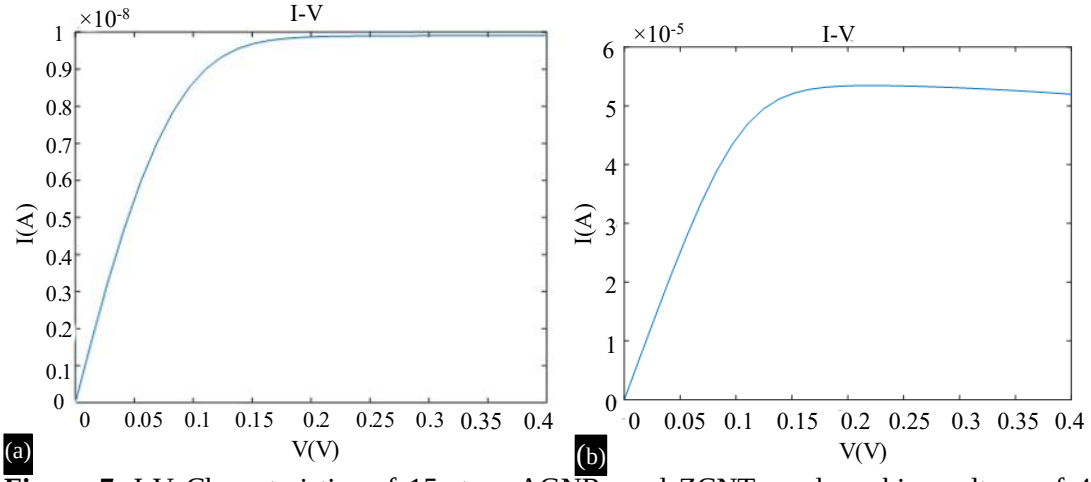

Figure 7. I-V Characteristics of 15-atom AGNRs and ZCNTs under a bias voltage of 400mV (a) 15AGNR, (b) 15-ZCNT.

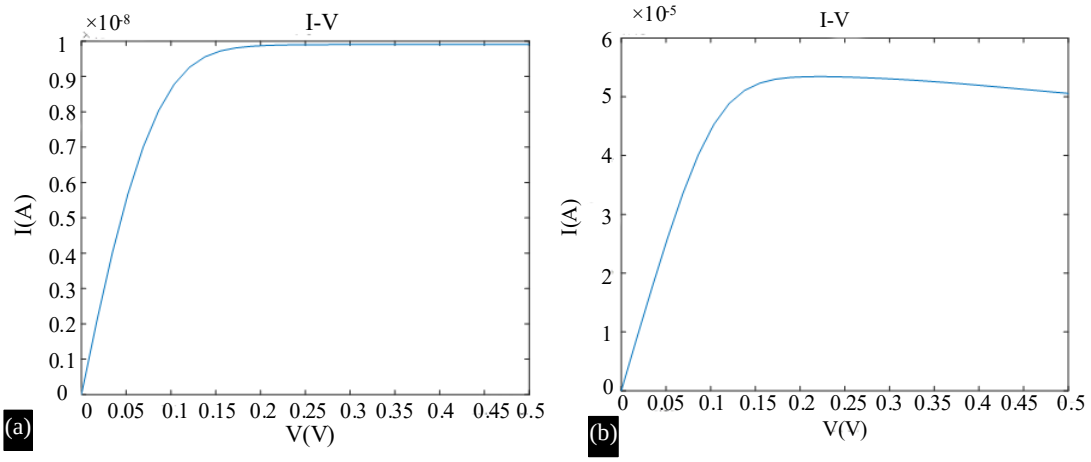

Figure 8. I-V Characteristics of 15-atom AGNRs and ZCNTs under a bias voltage of 500mV (a) 15-AGNR, (b) 15-ZCNT.

Figure 8 represents how the current behaves in 15-atom Armchair Graphene Nanoribbons (AGNRs) and 15-atom Zig-zag Carbon Nanotubes (ZCNTs) under a bias voltage of 500mV. As the voltage is applied, the current initially increase from zero for both the 15-atom AGNR and ZCNT [22]. For these specific 15-atom AGNRs and ZCNTs, the current-voltage (I-V) characteristics display a linear behaviour when subjected to a 500-millivolt bias, after reaching saturation point, the current stabilizes. This saturation current primarily determined by available conducting states within the AGNRs and ZCNTs. However, after reaching this saturation point, AGNRs maintain a constant current, while ZCNTs exhibit a further decrease in current or a reduction in the I-V curve with increasing voltage from 400 mV to 500 mV [23].

Figure 9 represents how the current behaves in 15-atom Armchair Graphene Nanoribbons (AGNRs) and 15-atom Zig-zag Carbon Nanotubes (ZCNTs) under a bias voltage of 600mV. As the voltage is applied, the current initially increase from zero for both the 15-atom AGNR and ZCNT. For these specific 15-atom AGNRs and ZCNTs, the current-voltage (I-V) characteristics display a linear behaviour when subjected to a 600-millivolt bias, after reaching saturation point, the current stabilizes. The available conducting states within the AGNRs and ZCNTs primarily determine this saturation current; however, once this saturation point is reached, AGNRs maintain a constant current, while ZCNTs show a further decrease in current or a reduction in the I-V curve with increasing voltage from 500 mV to 600 mV [24].

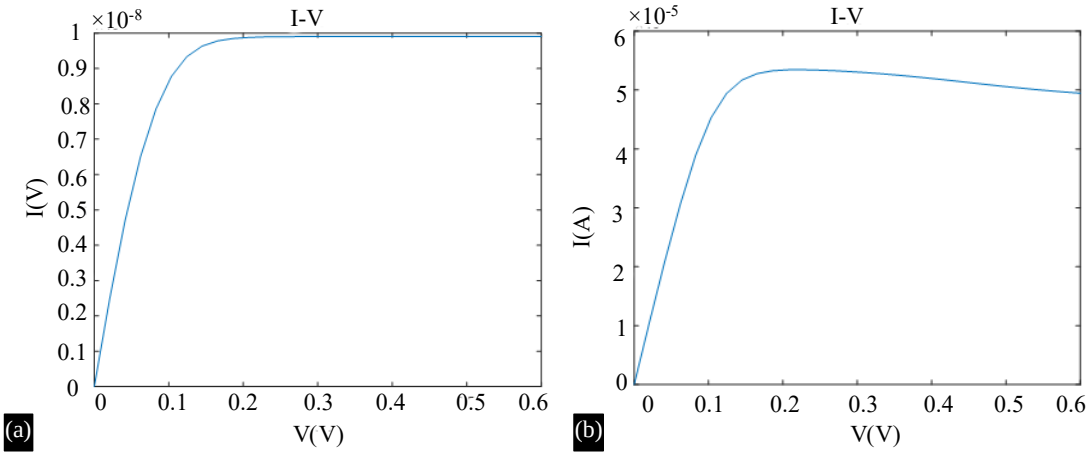

Figure 9. I-V Characteristics of 15-atom AGNRs and ZCNTs under a bias voltage of 600mV (a) 15AGNR, (b)15-ZCNT.

CONCLUSIONS

In this research, 15-atom armchair graphene nanoribbons (AGNRs) and 15-atom Zig-zag Carbon Nanotubes (ZCNTs) have been exposed to bias voltages of 100, 200, 300, 400, 500, and 600 millivolt levels by using Non-Equilibrium Green's Function approach. An interesting finding of the research is that, when materials with the same number of atoms are considered, AGNRs have significantly wider ribbon widths than ZCNTs. In addition, AGNRs have significantly higher bandgaps than ZCNTs, which is equal to zero. This suggests that ZCNTs require less energy for the movement of electrons from valence bands to conduction bands than do AGNRs.

The current-voltage (I-V) characteristics of AGNRs show linear behavior under 100 mV and 200 mV bias. However, at 300 mV, 400 mV, 500 mV, and 600 mV, there is no additional increase in current and a constant current flow is observed with an increase in voltage.Whereas for ZCNTs ZCNTs exhibit linear behavior at 100 mV and 200 mV, with current increasing with voltage. However, between 200 mV and 300 mV, the current does not increase with voltage.Following that, at 400 mV, 500 mV, and 600 mV, the current flow decreases while the voltages increase.The distinction between rising and declining behavior is caused by strong electron-electron interactions as well as the effects of quantum confinement. The results provide several prospects for the application of AGNRs and ZCNTs in the field of nano electronics and are significant for expanding our understanding of their electrical characteristics.

Furthermore, the study illustrates the effectiveness of the NEGF technique for evaluating the electrical properties of AGNRs and ZCNTs. The knowledge gathered from this research has the potential to affect the design of future electronic devices that use AGNRs and ZCNTs. Further research in this area is required to gain a thorough understanding of the electrical properties of AGNR and ZCNT, as well as find potential uses for these outstanding materials.

REFERENCES

1. Kadonoff, L., & Byam, G. (1989). Quantum Statistical Mechanics: Green's Function Method in Equilibrium and Nonequilibrium Problems.
2. Meir, Y., & Wingreen, N. S. (1992). Landauer formula for the current through an interacting electron region. *Physical review letters*, *68*(16), 2512.
3. Ferry, D., & Goodnick, S. M. (1999). *Transport in nanostructures* (No. 6). Cambridge university press.
4. Szałowski, K. (2015). Graphene nanoflakes in external electric and magnetic in-plane fields. *Journal of Magnetism and Magnetic Materials*, *382*, 318-327.

5. Szałowski, K. (2015). Graphene nanoflakes in external electric and magnetic in-plane fields. *Journal of Magnetism and Magnetic Materials*, *382*, 318-327.
6. Sadeghi, M. M., Pettes, M. T., & Shi, L. (2012). Thermal transport in graphene. *Solid State Communications*, *152*(15), 1321-1330.
7. Yin, Y., Zhang, Z., Zhong, H., Shao, C., Wan, X., Zhang, C., ... & Guo, Y. (2021). Tellurium nanowire gate-all-around MOSFETs for sub-5 nm applications. *ACS Applied Materials & Interfaces*, *13*(2), 3387-3396.
8. Zhou, M., Jin, H., & Xing, Y. (2020). In-plane dual-gated spin-valve device based on the zigzag graphene nanoribbon. *Physical Review Applied*, *13*(4), 044006.
9. Son, Y. W., Cohen, M. L., & Louie, S. G. (2006). Energy gaps in graphene nanoribbons. *Physical review letters*, *97*(21), 216803.
10. Wakabayashi, K., Takane, Y., Yamamoto, M., & Sigrist, M. (2009). Edge effect on electronic transport properties of graphene nanoribbons and presence of perfectly conducting channel. *Carbon*, *47*(1), 124-137.
11. Li, X., Wang, X., Zhang, L., Lee, S., & Dai, H. (2008). Chemically derived, ultrasmooth graphene nanoribbon semiconductors. *science*, *319*(5867), 1229-1232.
12. Yang, S., Li, D., Zhang, T., Tao, Z., & Chen, J. (2012). First-principles study of zigzag MoS2 nanoribbon as a promising cathode material for rechargeable Mg batteries. *The Journal of Physical Chemistry C*, *116*(1), 1307-1312.
13. S. M. Sze, *Electrons and Holes in Semiconductors*. New York: Wiley, 1969.
14. Wu, Q., Shen, L., Yang, M., Cai, Y., Huang, Z., & Feng, Y. P. (2015). Electronic and transport properties of phosphorene nanoribbons. *Physical Review B*, *92*(3), 035436.
15. Wakabayashi, K., Takane, Y., Yamamoto, M., & Sigrist, M. (2009). Electronic transport properties of graphene nanoribbons. *New Journal of Physics*, *11*(9), 095016.
16. Li, D., Wu, D., Zhang, X., Zeng, B., Li, M., Duan, H., ... & Long, M. (2018). The spin-dependent electronic transport properties of M (dcdmp) 2 (M= Cu, Au, Co, Ni) molecular devices based on zigzag graphene nanoribbon electrodes. *Physics Letters A*, *382*(21), 1401-1408.
17. Zhang, P., Li, X., Dong, J., Zhu, M., Zheng, F., & Zhang, J. (2022). π-magnetism and spin-dependent transport in boron pair doped armchair graphene nanoribbons. *Applied Physics Letters*, *120*(13).
18. Liu, L., Gao, J., Guo, X., & Zhao, J. (2013). Electromechanical properties of zigzag-shaped carbon nanotubes. *Physical Chemistry Chemical Physics*, *15*(40), 17134-17141.
19. Suzuki, S. (Ed.). (2013). *Syntheses and applications of carbon nanotubes and their composites*. BoD–Books on Demand.
20. Dresselhaus, G., Dresselhaus, M. S., & Saito, R. (1998). *Physical properties of carbon nanotubes*. World scientific.
21. Li, S., Zhang, X., Zhang, L., & Gao, M. (2010). Twinning-induced kinking of Sb-doped ZnO nanowires. *Nanotechnology*, *21*(43), 435602.
22. Gao, R., Wang, Z. L., & Fan, S. (2000). Kinetically controlled growth of helical and zigzag shapes of carbon nanotubes. *The Journal of Physical Chemistry B*, *104*(6), 1227-1234.
23. Xu, Z., & Buehler, M. J. (2009). Strain controlled thermomutability of single-walled carbon nanotubes. *Nanotechnology*, *20*(18), 185701.
24. Tian, B., Xie, P., Kempa, T. J., Bell, D. C., & Lieber, C. M. (2009). Single-crystalline kinked semiconductor nanowire superstructures. *Nature nanotechnology*, *4*(12), 824-829

